Vasodilator-Stimulated Phosphoprotein Biomarkers Are Associated with Invasion and Metastasis in Colorectal Cancer

$\circledS$SAGE

Giovanni M Pitari[1,2], Paolo Cotzia[3], Mehboob Ali[4], Ruth Birbe[5], Wendy Rizzo[3], Alessandro Bombonati[6], Juan Palazzo[3], Charalambos Solomides[3], Anthony P Shuber[2], Frank A Sinicrope[7] and David S Zuzga[2,8]

[1]Department of Pharmacology & Experimental Therapeutics, Thomas Jefferson University, Philadelphia, PA, USA. [2]BioDetego LLC, Philadelphia, PA, USA. [3]Department of Pathology, Thomas Jefferson University, Philadelphia, PA, USA. [4]Department of Pediatrics, The Research Institute at Nationwide Children's Hospital, Columbus, OH, USA. [5]Pathology Department, MD Anderson Cancer Center, Camden, NJ, USA. [6]Department of Pathology and Laboratory Medicine, Einstein Medical Center, Philadelphia, PA, USA. [7]Division of Medical Oncology and Comprehensive Cancer Center, Mayo Clinic, Rochester, MN, USA. [8]Department of Biology, La Salle University, Philadelphia, PA, USA.

ABSTRACT

BACKGROUND AND AIMS: The benefit of adjuvant chemotherapy for stage II colorectal cancer (CRC) patients remains unclear, emphasizing the need for improved prognostic biomarkers to identify patients at risk of metastatic recurrence. To address this unmet clinical need, we examined the expression and phosphorylation status of the vasodilator-stimulated phosphoprotein (VASP) in CRC tumor progression. VASP, a processive actin polymerase, promotes the formation of invasive membrane structures leading to extracellular matrix remodeling and tumor invasion. Phosphorylation of VASP serine (Ser) residues 157 and 239 regulate VASP function, directing subcellular localization and inhibiting actin polymerization, respectively.

METHODS: The expression levels of VASP protein, pSer^{157}-VASP, and pSer^{239}-VASP were determined by immunohistochemistry in tumors and matched normal adjacent tissue from 141 CRC patients, divided into 2 cohorts, and the association of VASP biomarker expression with clinicopathologic features and disease recurrence was examined.

RESULTS: We report that changes in VASP expression and phosphorylation were significantly associated with tumor invasion and disease recurrence. Furthermore, we disclose a novel 2-tiered methodology to maximize VASP positive and negative predictive value performance for prognostication.

CONCLUSION: VASP biomarkers may serve as prognostic biomarkers in CRC and should be evaluated in a larger clinical study.

KEYWORDS: Colorectal cancer, vasodilator-stimulated phosphoprotein, actin cytoskeleton, invasion, metastasis

Colorectal cancer (CRC) is the second leading cause of cancer-related death in the United States. In 2017, ~100 000 patients are expected to be diagnosed with local (stages 0-II) or regional (stage III) CRC where prognostic information is needed to guide patient management.[1] Unfortunately, current histopathologic staging methods are imperfect and considerable stage-independent variability exists in clinical outcome. The role of adjuvant chemotherapy in stage II patients remains unresolved,[2–9] and it is estimated that one-third of such patients receive adjuvant chemotherapy in the United States. Accordingly, a substantial proportion of patients are currently overtreated and a high-risk subset is undertreated.[10] Acknowledging the limitations of stage-specific treatment guidelines, there remains an unmet need for more accurate prognostic tools to identify stage II patients at risk of relapse that are likely to benefit from adjuvant chemotherapy.[11]

Prognostic test development is predicated on the identification of novel biomarkers associated with tumor recurrence/metastasis. Actin-binding proteins such as the vasodilator-stimulated phosphoprotein (VASP) represent promising biomarker targets with potential prognostic utility.[12–15] VASP is an actin polymerase that directs the formation of migratory and invasive membrane structures including filopodia and invadopodia.[12] VASP function is regulated by post-translational modifications, where phosphorylation at Ser^{157} (pSer^{157}-VASP) affects intracellular localization, and phosphorylation at Ser^{239} (pSer^{239}-VASP) inhibits invasive cell morphology and a metastatic phenotype.[12,13] Notably, VASP Ser phosphorylation is

Table 1. Clinicopathologic parameters of CRC patients in TMA study.

Age (y)	
Median (range)	66 (28-91)
Sex (%)	
Male	56 (47.1)
Female	61 (51.2)
ND	2 (1.7)
Race (%)	
Caucasian	67 (56.3)
African American	43 (36.1)
Hispanic	3 (2.5)
ND	6 (5.1)
Tumor site (%)	
Right colon	46 (38.6)
Transverse colon	9 (7.6)
Left colon	37 (31.1)
Sigmoid	17 (14.3)
ND	10 (8.4)
TNM stage[a] (%)	
0 (Tis, N0M0)	12 (10.1)
I (T1-2, N0M0)	24 (20.2)
IIA (T3, N0M0)	11 (9.2)
IIB (T4, N0M0)	20 (16.8)
IIIA (T1-2, N1M0)	12 (10.1)
IIIB (T3-4, N1M0)	12 (10.1)
IIIC (T1-4, N2M0)	13 (10.9)
IV (T1-4, N0-2, M1)	15 (12.6)
Differentiation grade (%)	
Well	9 (7.6)
Moderate	82 (68.9)
Poor	12 (10.1)
ND	16 (13.4)
Lymph node metastasis (%)	
Yes (N+)	37 (35.6)
No (N0)	67 (64.4)
Distant metastasis (%)	
Yes (M+)	15 (12.6)
No (M0)	104 (87.4)

Abbreviations: CRC, colorectal cancer; ND, not determined; TMA, tissue microarray.
[a]TNM annotations indicate Tis, limited to mucosa (carcinoma in situ); T1, limited to submucosa; T2, invading the muscularis propria; T3, invading the serosa; T4, invading adjacent organs; N0, no lymph nodes involvement; N1, metastasis in 1 to 3 lymph nodes; N2, metastasis in ≥4 lymph nodes; M0, no distant metastasis; M1, metastasis at distant organs.

associated with aggressiveness in breast cancer and is reduced in human CRC, suggesting that dysregulated VASP phosphorylation during colorectal transformation may underlie the metastatic phenotype.[12,14]

In this report, we examined the relationship between VASP, pSer[157]-VASP, and pSer[239]-VASP in primary human CRC tumors with disease progression. Tissue microarrays (TMAs) containing 119 primary CRC tumors and matched normal adjacent tissue (NAT) specimens were subjected to immuno-histochemistry (IHC) for each VASP biomarker (VASP, pSer[157]-VASP, or pSer[239]-VASP), and semi-quantitative scoring was performed by pathologists blinded to clinical data (0-3 scale; Table 1 and Supplementary Figure 1A). Compared with matched NATs, tumors exhibited significant expression changes in VASP (upregulation) and pSer[157]-VASP (down-regulation; Figure 1A). However, following normalization, where staining intensity scores for pSer[157]-VASP and pSer[239]-VASP were divided by the score for VASP, both phosphorylated VASP forms were significantly downregulated in adenocarcinomas compared with matched NAT, or compared with non-matched carcinoma in situ (Figure 1B). Moreover, analysis of normalized relative levels (Tumor/NAT) of VASP phosphorylated forms revealed that pSer[239]-VASP was also significantly decreased in lymph node positive (N+) compared with node negative (N0) CRCs (Figure 1C). These data suggest that differential expression of VASP and its phosphorylated forms are associated with CRC invasion and metastasis to regional lymph nodes.

To investigate potential clinical utility of VASP biomarkers, a pilot study was performed employing tissues from 22 stage II (T3N0) CRC patients comprising primary tumors and matched NATs (mounted as whole-tissue sections). Expression of VASP biomarkers was analyzed in relationship to clinical outcome data (≥5 year follow-up). The patient cohort was selected as chemotherapy-naive, well-balanced for tumor site and grade distribution, and enriched for tumor recurrence (55%; Table 2). Following IHC staining for VASP, pSer[157]-VASP, or pSer[239]-VASP, a semi-quantitative H-scoring system was employed (Supplementary Figure 1B). Independent scores from 2 blinded pathologists were highly correlated, suggesting that staining intensity quantification of VASP biomarkers is a reliable and objective measurement (Supplementary Figure 2). Importantly and compared with NATs, tumors exhibited significant upregulation of VASP and downregulation of absolute or VASP-normalized levels of both pSer[157]-VASP and pSer[239]-VASP (Figure 2A), confirming the observations from TMA studies. Then, VASP-normalized values of pSer[157]-VASP and pSer[239]-VASP, and relative tumor/NAT ratios of each VASP biomarker were calculated and Receiver Operating Characteristic (ROC) analysis performed to identify threshold values that optimally discriminate between recurrence and recurrence-free survival (Supplementary Figure 3). Furthermore, hazard ratios (HRs) and 95% confidence intervals (CIs) were
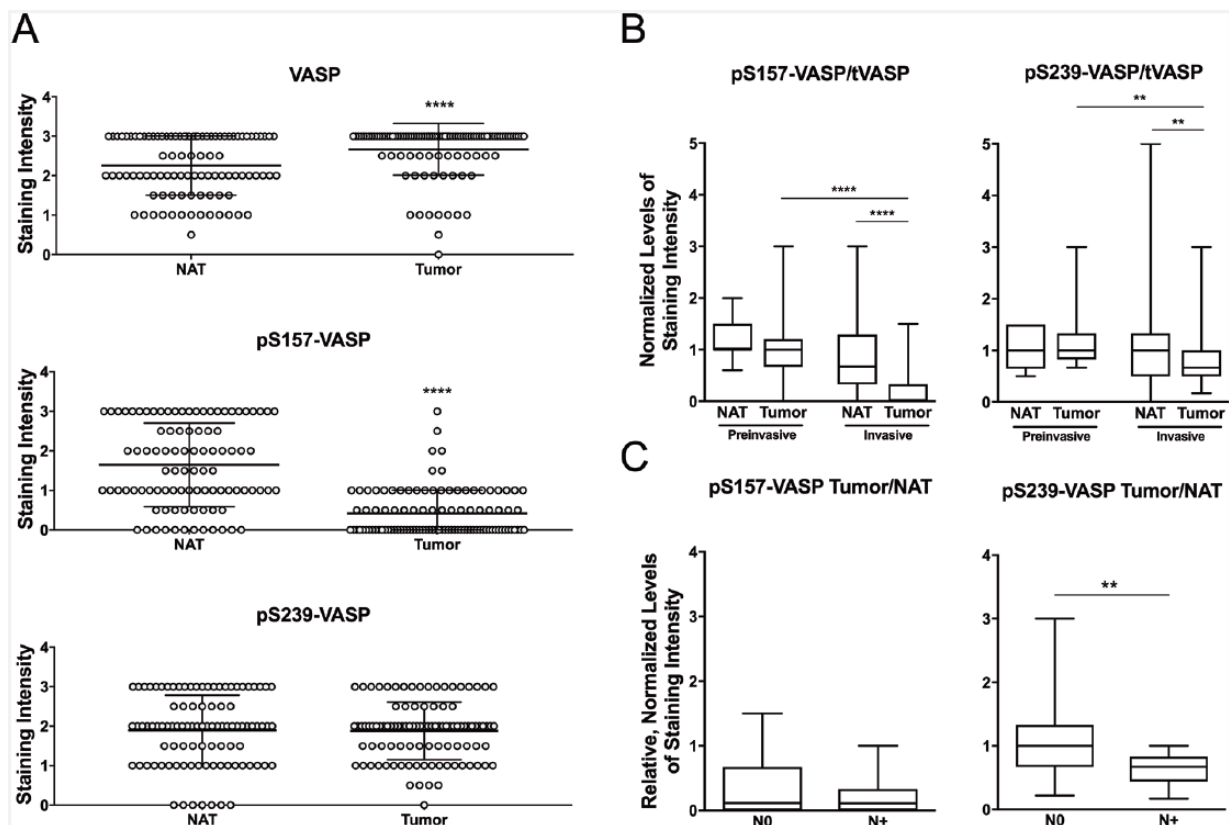
Figure 1. (A) Scatter plots indicate IHC scoring for VASP (n=93), pSer[157]-VASP (n=94), and pSer[239]-VASP (n=94) and include individual values of matched tumor and NAT pairs. Mean values with standard deviation are indicated. ****$P<.0001$ by 2-tailed, paired *t*-test. (B) IHC scoring for VASP-normalized ratios of pSer[157]-VASP (*left panel*) in carcinomas in situ (n=9) and matched NAT (n=11), and adenocarcinoma tumors (n=101) and matched NAT (n=93), or pSer[239]-VASP (*right panel*) in preinvasive tumor (n=9) and matched NAT (n=11), and invasive tumor (n=100) and matched NAT (n=95). Box and whisker plots indicate median values and include 25th to 75th percentiles. For preinvasive to invasive comparisons, ****$P<.0001$; **$P=.003$ by 2-tailed, unpaired *t*-test. For tumor to NAT comparisons, only tissues with matched tumor and NAT were included in the analysis. ****$P<.0001$; **$P=.001$ by 2-tailed, paired *t*-test. (C) Staining intensity ratios of VASP-normalized pSer[157]-VASP (*left panel*) or pSer[239]-VASP (*right panel*) in tumors over matched NAT (TNM stages I-III). Box and whisker plots are as described above. N of tissues quantified were pSer[157]-VASP/VASP (Tumor/NAT), 46 (N0) and 27 (N+); pSer[239]-VASP/VASP (Tumor/NAT), 44 (N0) and 27 (N+). **$P<.002$ by 2-tailed, unpaired *t*-test. IHC indicates immunohistochemistry; NAT, normal adjacent tissue; VASP, vasodilator-stimulated phosphoprotein.

calculated using Cox proportional hazard models and Kaplan-Meier survival curves were generated (Figure 2B and Supplementary Figure 3). VASP-normalized pSer[157]-VASP and pSer[239]-VASP values in tumors, but not NAT, significantly discriminated by recurrence and recurrence-free survival among the cohort, with HRs undefined for pSer[157]-VASP (due to absence of recurrence in the low-risk group), and of 3.6 (95% CI, 0.9-14.3; $P=.02$) for pSer[239]-VASP (Supplementary Figure 3A and Figure 2B). Relative tumor/NAT values of pSer[157]-VASP and pSer[239]-VASP, but not VASP, also significantly discriminated patient risk groups (Supplementary Figure 3B) and exhibited HRs of 6.3 (95% CI, 1.9-21.4; $P=.04$) and 7.6 (95% CI, 2.3-25; $P=.02$), respectively (Figure 2B). Unlike VASP biomarkers, no significant associations were observed between traditional clinicopathological parameters, including age, sex or primary tumor site (Figure 2B). Importantly, integration of multiple VASP biomarker ratios into algorithms provided single index scores that were found to more accurately

discriminate between recurrence and recurrence-free survival than did individual ratios. ROC analysis of one such algorithm (Supplementary Figure 3C) resulted in an optimally discriminating threshold (area under the curve [AUC]=0.83; 95% CI, 0.63-1.02; $P=.009$) with an HR of 12.4 (95% CI, 3.8-40.6; $P=.002$; Figure 2B).

Finally, VASP biomarker ratios were applied in sequence, employing a novel, 2-tiered model developed to optimize negative and positive predictive values (NPV, PPV) (Figure 2C). Here, a Tier 1 stratification is applied based on optimization of NPV. Low risk patients identified by Tier 1 are then excluded from Tier 2 stratification. In this way, true negative depletion and the subsequent increased incidence of true positives in the Tier 2 cohort introduce a bias for higher PPV performance. VASP-normalized pSer[157]-VASP tumor ratio was selected as the Tier 1 test based on the high NPV exhibited (100%), while the pSer[239]-VASP tumor/NAT ratio (PPV, 72%) was employed in Tier 2. As predicted, the PPV performance of the Tier 2

Table 2. Clinicopathologic parameters of CRC patients in whole-tissue section study.

Age (y)	
Median (range)	62 (48-81)
Sex (%)	
Male	12 (54.5)
Female	10 (45.5)
Race (%)	
Caucasian	20 (90.9)
ND	2 (9.1)
Tumor site (%)	
Right colon	5 (22.7)
Transverse colon	5 (22.7)
Left colon	3 (13.7)
Sigmoid	9 (40.9)
TNM stage[a] (%)	
IIA (T3, N0M0)	22 (100)
Differentiation grade (%)	
Well	4 (18.2)
Moderate	17 (77.3)
Poor	1 (4.5)
Lymph nodes examined	
Median (range)	21.5 (8-44)
Chemotherapy (%)	
Yes	0 (0)
No	22 (100)

Abbreviations: CRC, colorectal cancer; ND, not determined.
[a]TNM annotations indicate T3, invading the serosa; N0, no lymph node involvement; M0, no distant metastasis.

VASP test greatly improved (to 91%) following patient (n, 6) exclusion in Tier 1 (Figure 2C).

Altogether, these observations suggest that VASP biomarkers are associated with disease progression and recurrence risk in CRC patients, and may be configured to optimize clinically relevant measures such as NPV and PPV. Future independent validation studies that use large patient cohorts are needed to fully evaluate and demonstrate the prognostic value of VASP biomarkers in CRC.

Materials and Methods

Patients

For the TMAs, paraffin-embedded colorectal adenocarcinomas and respective NATs from 119 patients homogeneously

distributed along TNM pathological stages were obtained from the Department of Pathology, Anatomy and Cell Biology at Thomas Jefferson University (Philadelphia, PA), under a protocol approved by the Institutional Review Board (IRB). Tissue blocks, sorted by TNM stage, were processed and correspondent tissue cores of 0.7 mm in diameter were collected from regions of interest and assembled in duplicate into 2 TMA blocks, TMA-1 and TMA-2, containing a total of 150 and 118 cores, respectively (see below for detail). For whole-tissue section studies, clinical residual tissues from 22 stage II, T3 patients with matched colon adenocarcinomas and NAT (mounted as whole-tissue sections) and clinical outcomes data (≥5 year follow-up) were obtained from the Mayo Clinic under an IRB-approved protocol.

Tissue microarrays

Each TMA block contained 2 tissue sectors, the *Tumor* grid and the correspondent *NAT* grid (Supplementary Figure 1). TMA-1 was constructed with 67 low TNM stage cases (from top-to-bottom: 12 stage 0, 24 stage I, and 31 stage II), while TMA-2 contained 52 high TNM stages (from top-to-bottom: 37 stage III and 15 stage IV). Normal colorectal tissue controls from non-cancer patients were also allocated (in duplicate) in the first 6 positions (from top left corner) of each tissue sector, and served as the internal positive controls. Moreover, 10 (in TMA-1) and 8 (in TMA-2) tissue cores from human placenta from de-identified donors were allocated in vertical positions in the middle (number 7) column, starting from the second row, of each sector and served as the negative control samples. Then, 4 μm tissue sections were cut from each TMA, mounted on microscope slides and subjected to IHC. Following standard pathological processing, insufficient or poorly processed tissue cores resulted in 2 (1.7%) patients lacking any relevant tissue, and 20 (16.8%) cases with 1 to 3 missing core pairs (in Tumor and/or NAT). Incomplete cases were also included in the analyses, which consequently translated in different total numbers of each biomarker evaluated (as indicated in legends to figures).

Immunohistochemistry

IHC staining was performed with antibodies to human VASP (SC-46668, Santa Cruz, Santa Cruz, CA), pSer[157]-VASP (SC101818, Santa Cruz), or pSer[239]-VASP (SAB4300129, Sigma Aldrich, St. Louis, MO). Following sequential steps of deparaffinization, rehydratation, and antigen retrieval, TMA slides were subjected to serial incubations with primary antibodies (VASP, 1:1000; pSer[157]-VASP, 1:100; pSer[239]-VASP, 1:500), appropriate secondary antibodies, and the DAB reporter system (Vector Laboratory, Burlingame, CA). Then, the membranous and cytoplasmic staining intensity of each VASP marker (evaluated in epithelial cell compartments only) was semiquantitatively scored by 2 blinded clinical
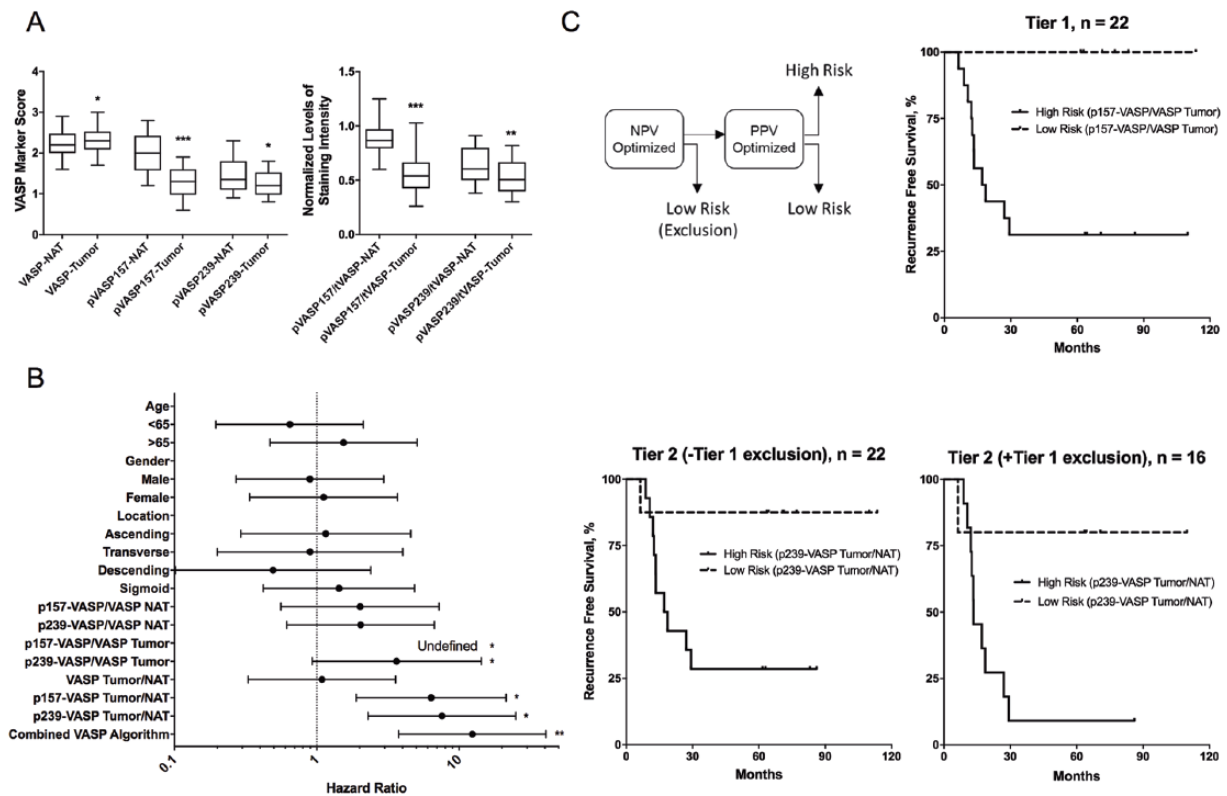
Figure 2. (A) Box and whisker plots of IHC scoring for individual biomarkers (*left panel*) or VASP-normalized ratios of pSer[157]-VASP and pSer[239]-VASP (*right panel*). ****$P < .0001$; **$P = .003$; *$P < .05$ by 2-tailed, paired *t*-test. (B) HRs for recurrence and 95% CIs associated with traditional pathological parameters and VASP biomarkers. **$P = .002$; *$P < .05$ by log-rank (Mantel-Cox) test. (C) Diagram of 2-tiered testing model (*upper left panel*). Kaplan-Meier survival curves associated with the Tier 1 prognostic biomarker VASP-normalized pSer[157]-VASP (*upper right panel*), and the Tier 2 prognostic biomarker pSer[239]-VASP tumor/NAT, before (*lower left panel*) and after (*lower right panel*) patients' exclusion by Tier 1 testing. CI indicates confidence interval; IHC, immunohistochemistry; HR, hazard ratio; NAT, normal adjacent tissue; VASP, vasodilator-stimulated phosphoprotein.

pathologists on a 0-to-3 scale (0, absent; 1, weak; 2, moderate; 3, strong).

In the whole-tissue section study, slides were processed using the Bond Polymer Refine Detection (DS9800, Leica) staining kit on a Bond automated stainer (Leica). IHC was performed according to the following conditions: VASP, 1:3000 (with BOND Epitope Retrieval Solution 2); pSer[157]-VASP, 1:200 (with BOND Epitope Retrieval Solution 2); and pSer[239]-VASP, 1:500 (with BOND Epitope Retrieval Solution 1). Levels of VASP biomarkers in epithelial membranous and cytoplasmic compartments were calculated semiquantitatively by 2 blinded clinical pathologists as H-scores, that measure staining intensity (0, absent; 1, weak; 2, moderate; 3, strong) in combination with the percentage of cells staining positively (H-score = [3 × %cells] + [2 × %cells] + [1 × %cells]).

Statistical analysis

Comparisons of VASP biomarker expression in Tumor versus NAT, invasive versus preinvasive lesions, or N+ versus N0 disease were evaluated by 2-sided Student *t* tests. Pathologists' H-scoring comparisons were evaluated with the Spearman Correlation test. Receiver operating characteristic analysis was employed to determine optimal thresholds that discriminated low-risk and high-risk patients, and time to recurrence was analyzed using the Kaplan-Meier estimator of the survival curves. Test-positive patients had documented disease recurrence and test-negative patients were defined as recurrence-free for ≥5 years following initial surgery, and were censored on the date of last follow-up. The difference in time to recurrence between test-negative and test-positive patients was evaluated using the 2-sided log-rank test. Cox proportional hazard models were used to determine HRs and 95% coefficient intervals (Cis). The algorithm, $\sqrt{(pSer^{157}\text{-VASP Tumor/NAT} \times pSer^{239}\text{-VASP Tumor/NAT})} / (\text{VASP Tumor/NAT})^2$, provided a single index score to evaluate combined biomarker ratios. All statistical analyses were performed with GraphPad Prism software (Version 7).

Author Contributions

DSZ and GMP contributed to the study concept and design, analysis and interpretation of data, drafting of the manuscript, statistical analysis, administrative support, and study supervision. PC, MA, WR, AB, JP, and CS contributed to the acquisition of data and technical supervision. APS contributed to the analysis and interpretation of data and critical and intellectual

revision of the manuscript. FAS contributed to the study concept and design and acquisition of data. All authors had access to the study data and had reviewed and approved the final manuscript.

REFERENCES

1. Surveillance, Epidemiology, and End Results (SEER) Program. www.seer.cancer.gov.
2. Efficacy of adjuvant fluorouracil and folinic acid in colon cancer. International Multicentre Pooled Analysis of Colon Cancer Trials (IMPACT) investigators. *Lancet*. 1995;345:939–944.
3. Efficacy of adjuvant fluorouracil and folinic acid in B2 colon cancer. International Multicentre Pooled Analysis of B2 Colon Cancer Trials (IMPACT B2) investigators. *J Clin Oncol*. 1999;17:1356–1363.
4. Schrag D, Rifas-Shiman S, Saltz L, Bach PB, Begg CB. Adjuvant chemotherapy use for Medicare beneficiaries with stage II colon cancer. *J Clin Oncol*. 2002; 20:3999–4005.
5. Gill S, Loprinzi CL, Sargent DJ, et al. Pooled analysis of fluorouracil-based adjuvant therapy for stage II and III colon cancer: who benefits and by how much? *J Clin Oncol*. 2004;22:1797–1806.
6. Gray R, Barnwell J, McConkey C, Hills RK, Williams NS, Kerr DJ ; Quasar Collaborative Group. Adjuvant chemotherapy versus observation in patients with colorectal cancer: a randomised study. *Lancet*. 2007;370:2020–2029.
7. Hutchins G, Southward K, Handley K, et al. Value of mismatch repair, KRAS, and BRAF mutations in predicting recurrence and benefits from chemotherapy in colorectal cancer. *J Clin Oncol*. 2011;29:1261–1270.
8. Tournigand C, André T, Bonnetain F, et al. Adjuvant therapy with fluorouracil and oxaliplatin in stage II and elderly patients (between ages 70 and 75 years) with colon cancer: subgroup analyses of the Multicenter International Study of Oxaliplatin, Fluorouracil, and Leucovorin in the Adjuvant Treatment of Colon Cancer trial. *J Clin Oncol*. 2012;30:3353–3360.
9. Wu X, Zhang J, He X, et al. Postoperative adjuvant chemotherapy for stage II colorectal cancer: a systematic review of 12 randomized controlled trials. *J Gastrointest Surg*. 2012;16:646–655.
10. Chagpar R, Xing Y, Chiang YJ, et al. Adherence to stage-specific treatment guidelines for patients with colon cancer. *J Clin Oncol*. 2012;30:972–979.
11. Meropol NJ. Ongoing challenge of stage II colon cancer. *J Clin Oncol*. 2011; 29:3346–3348.
12. Zuzga DS, Pelta-Heller J, Li P, Bombonati A, Waldman SA, Pitari GM. Phosphorylation of vasodilator-stimulated phosphoprotein Ser239 suppresses filopodia and invadopodia in colon cancer. *Int J Cancer*. 2012;130:2539–2548.
13. Döppler H, Storz P. Regulation of VASP by phosphorylation: consequences for cell migration. *Cell Adh Migr*. 2013;7:482–486.
14. Döppler H, Bastea L, Borges S, Geiger X, Storz P. The phosphorylation status of VASP at serine 322 can be predictive for aggressiveness of invasive ductal carcinoma. *Oncotarget*. 2015;6:29740–29752.
15. Oudin MJ, Hughes SK, Rohani N, et al. Characterization of the expression of the pro-metastatic Mena(INV) isoform during breast tumor progression. *Clin Exp Metastasis*. 2016;33:249–261.